Quadricyclane Radical Cation Q^+: Formation and Isomerization in Liquid Methylcyclohexane

Rolf E. Bühler* and Murat A. Quadir†

Laboratory for Physical Chemistry, ETH Zürich, Switzerland

Received: October 18, 1999; In Final Form: January 4, 2000

The radical cation of quadricyclane (Q) was studied by pulse radiolysis at 133 K with methylcyclohexane (MCH) as solvent, saturated with N_2O. The known solvent radical cations, MCH^+ and its precursor M^{+*}, are expected to produce Q^+ by charge transfer. Although Q^+ was known not to absorb in the visible λ-range, there was a very early absorption band at $\lambda_{max} = 720$ nm (the transient is called Q^{+*}), which eventually transformed into the cation of norbornadiene (NBD^+) with $\lambda_{max} = 650$ nm. The analysis of the geminate ion kinetics with the semiempirical $t^{-0.6}$ kinetic law revealed that Q^{+*} decays faster than the isomer NBD^+ is built up. Q^{+*} must be a precursor to the nonabsorbing Q^+, which eventually isomerizes to NBD^+, followed by a back reaction with Q to re-form Q^+. The quantitative analysis revealed that a substantial amount of the cations is lost before NBD^+ is formed. This loss to a fragment or isomer (called F^+) occurs from Q^{+*}. As this loss dropped drastically for very low [Q], Q^{+*} must increasingly be bypassed by lowering [Q]. It turns out that Q^{+*} is produced from M^{+*} only (the higher energy precursor of the solvent radical cation MCH^+) in competition with the transformation of M^{+*} to MCH^+, the latter becoming dominant at low [Q], increasingly producing Q^+ directly from MCH^+ without going through Q^{+*}. The loss yield (F^+) correspondingly loses. The complete mechanism is given (Scheme 3). All the rate constants and the free ion contributions of all cations were determined and, together with the known G_{fi} value, the absorption coefficients were derived. Comparing these results with a mechanism proposed recently by Adam et al. (*J. Am. Chem. Soc.* **1995**, *117*, 9693) suggests that Q^{+*} corresponds to their cation $Q^+(l)$, where the lateral bonds are oxidized, Q^+ to their cation $Q^+(i)$, where the internal bonds are oxidized, and F^+ to the Q^+ isomer BHD^+ (the bicyclo[3.2.0]hepta-2,6-diene cation). The precursor ion M^{+*} of the solvent, which is responsible for the Q^{+*} production must be of higher energy than MCH^+; however, its structure remains unknown. The two precursor cations, M^{+*} and Q^{+*}, are critically compared and discussed.

I. Introduction

Ionic processes in nonpolar solvents are usually complex as they follow dominantly nonhomogeneous kinetics with only very small free ion contributions. This is particularly true for alkanes at low temperatures.

The method to analyze such nonhomogeneous geminate ion kinetics, initiated by pulse radiolysis, is based on the semiempirical $t^{-0.6}$ kinetic law[1] (see below), which has been extended to cover ion−molecule reactions and unimolecular ionic processes as well. With this theory we reached a rather good understanding for the cations of the solvent methylcyclohexane (MCH) with the radical cation MCH^+ [2] and its precursor M^{+*} [3] (see discussion at the end of the paper).

So far we limited ourselves to apply the $t^{-0.6}$ theory to the solvent MCH only, to understand the validity limits of the theory. Selected solutes were chloroform for anion studies ($CHCl_3^-$ fragmentation[4]) and norbornadiene (NBD), *cis*- and *trans*-decalin, and adamantane[5] for cation studies. In analogy to NBD, its isomer quadricyclane (Q) should also act as a positive charge scavenger from MCH^+ and M^{+*} (I_p(MCH) = 9.85 eV, I_p (NBD) = 8.43 eV, and I_p(Q) 7.85 eV).

There is a large literature on the cation of Q, one of the latest being from Adam et al.[6] The existence of Q^+ has been proven by ESR[7] and was proposed as an intermediate in many papers, e.g., in CIDNP studies[8] and in pulse radiolysis.[9] It was known that a complex isomerization mechanism is involved. Unfortunately, quantum chemistry predicts[10] that Q^+ should only absorb in the UV region ($\lambda \leq 310$ nm), therefore badly overlapping with other transient absorptions.

From our pulse radiolysis results for Q in MCH it became quickly clear that not only is a complex mechanism involved, but there is also an early, rather puzzling, 720 nm transient absorption, which eventually converts into a band at 650 nm, known to be due to NBD^+. The interest in this paper therefore focuses on the following points: (1) to understand the isomerizations with Q^+ and NBD^+, the identity of the 720 nm species, and the complete ionic mechanism, (2) to improve our understanding of radical cations of alkanes, in comparison with the solvent cation MCH^+ and its precursor M^{+*}, and (3) to gain experience for the applicability of the $t^{-0.6}$ kinetic law to complex, nonhomogeneous systems.

The original $t^{-0.6}$ *kinetic law*[11] describes the probability of survival of the geminately recombining ions relative to the free ion yield:

$$\frac{G(t)}{G_{fi}} = 1 + \underbrace{0.6\left[\frac{r_c^2}{D}\right]^{0.6}}_{\alpha} t^{-0.6} = \frac{\text{absorbance}(t)}{\text{absorbance}(\infty)} = \frac{A(t)}{IA} \qquad (1)$$

* To whom correspondence should be addressed at Physical Chemistry, ETH Zürich, Mühlebachstr. 96, 8008 Zürich, Switzerland.

† Present address: Nalco Chemical Co., One Nalco Center, Naperville, IL 60563-1198.

10.1021/jp993707k CCC: $19.00
Published on Web 03/08/2000

The absorption may have contributions from both types of ions (sum of both absorption coefficients). Any plot of the absorbance $A(t)$ against $t^{-0.6}$ should be linear. Its intercept IA for $t = \infty$ ($t^{-0.6} = 0$) corresponds to the absorbance of the free ion yield. The slope divided by the intercept IA is called α (or β, γ, etc.). From this value, with the known Onsager radius r_c, an experimental diffusion constant can be derived: $D_{exp} = D^+ + D^-$. Theoretical support for the $t^{-0.6}$ rate law was recently given by Barczak and Hummel.[12] From the many semiempirical theories to simulate the nonhomogeneous, geminate ion kinetics, only the $t^{-0.6}$ rate law is able to explain the experimental results in methylcyclohexane.[2,13]

If a geminate ion reacts (in addition to ion recombination), there is a change from a primary to a secondary pair of geminate ions, with a first-order or pseudo-first-order rate constant, k_1.[2,3] The primary geminate ion kinetics is given by

$$\frac{A_{prim}(t)}{IA} = [1 + \alpha t^{-0.6}]e^{-k_1 t} \qquad (2)$$

$$\alpha = 0.6\left[\frac{r_c^2}{D_{prim}}\right]^{0.6} \quad \text{and} \quad IA = A_{prim}(\infty)$$

The secondary geminate ion kinetics may be approximated by

$$\frac{A_{sec}(t)}{IB} = [1 + \beta t^{-0.6}][1 - e^{-k_1 t}] \qquad (3)$$

$$\beta = 0.6\left[\frac{r_c^2}{D_{sec}}\right]^{0.6} \quad \text{and} \quad IB = A_{sec}(\infty)$$

The sum of primary and secondary ion absorbances then simulates the experimental time profile

$$A(t) = A_{prim}(t) + A_{sec}(t) \qquad (4)$$

The application of this $t^{-0.6}$ simulation to systems where geminate ion recombination kinetics is complicated by simultaneous ionic reactions was critically discussed in recent papers by Bühler.[1,14] Due to its simplicity, it is a very powerful tool to study geminate ion mechanisms.

As M^{+*} not only relaxes to MCH^+ but also fragments to a cation of methylcyclohexene ($MCHene^+$),[2] such parallel ionic reactions do yield mixed pairs of secondary ions ($MCHene^+$/$Anion^-$ and MCH^+/$Anion^-$), in this case with quite different mobilities. The geminate recombination kinetics of such mixed ion pairs still follows a linearity against $t^{-0.6}$; however, the mobility values (α, β, etc.) become λ-dependent,[4] if the pairs represent different mobilities. In this paper, however, the solute cations (Q^{+*} (see below), Q^+, and NBD^+) and the anion (N_2O^- or O^-) are all diffusional and therefore of the same mobility.

II. Experimental Section

The technique of pulse radiolysis with a Febetron 705 accelerator (Physics International) for 30 ns pulses of 2 MeV electrons has been used as reported.[2,3] Experiments with MCH as solvent were performed at 133 K in the liquid state. The stainless steel cell had an optical path length of 2 cm. A typical dose was between 50 and 150 Gy. Dosimetry was done by calorimetry. All data usually are normalized to 100 Gy. The data treatment, kinetic analysis, and data simulation were performed on a PDP 11/73 computer.

All the experimental signals were corrected for the cell window signal (quartz defects) as described in the previous paper.[2] The origin of shock waves in pulse radiolysis cells and the method to minimize the effect have also previously been discussed in detail.[2,15] As the shock waves are correlated with the speed of sound and are reflected back and forth in the cell, the shock pattern can be identified as periodic signals during earlier times, but which get smeared out later on.

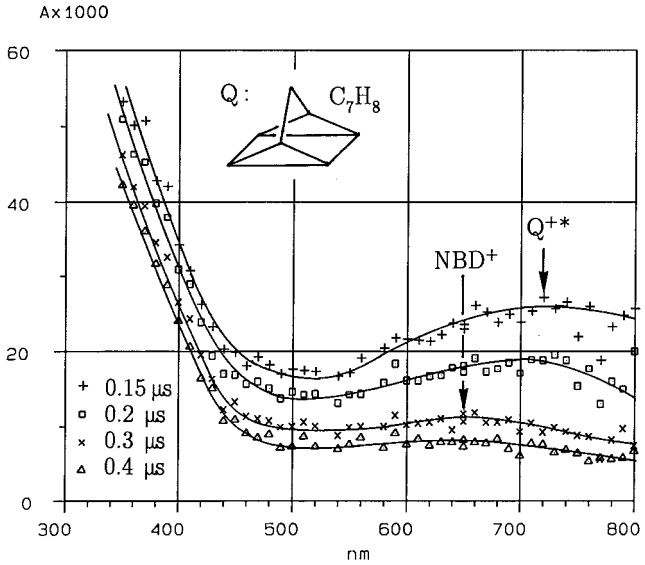

Figure 1. Transient spectra in a solution of 100 mM Q in MCH at 133 K. Absorbance *A* normalized to 100 Gy.

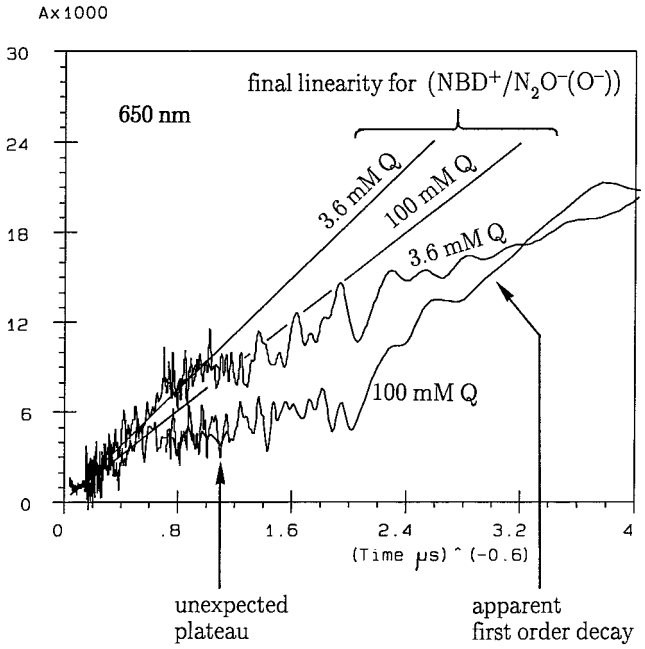

Figure 2. $t^{-0.6}$ plot of typical rate curves at 650 nm for Q in MCH (133 K) at high concentration ([Q] = 100 mM) and low concentration ([Q] = 3.6 mM) to illustrate the [Q]-dependent behavior. The final linearities are also [Q]-dependent, due to viscosity variation, as found previously for NBD.[2]

Chemicals. MCH (Fluka purum, >98%, GC) was passed through a column of aluminum oxide, dried over molecular sieves A4, and then fractionated through a Fischer "Spaltrohrkolonne" with about 30 theoretical plates. Quadricyclane (quadricyclo[2.2.1.0.^{2,6}.0^{3,5}]heptane, Aldrich, 99%) and N_2O (PanGas, 99%, Luzerne CH) were used as received.

III. Results

Pulse radiolysis of a solution of Q in MCH (N_2O saturated) at 133 K (a supercooled liquid with $\eta \approx 1.26$ Pa s) revealed

TABLE 1: Results from the $t^{-0.6}$ Kinetic Simulation

[Q] (mM)	$\alpha = \beta = \gamma$[a] ($\mu s^{0.6}$)	$\bar{k}_1/10^6$ [b] (s^{-1})	$\bar{k}_s/10^5$ [b] (s^{-1})	k_s/k_{iso}[c]	IC_{tot} (%) (total free ion yield, Q^+/NBD^+ channel)
200	27.0	7.25 ± 0.35	10.5 ± 0.7	1.36	46.4 ± 3.0
100	26.7	5.33 ± 0.26	9.17 ± 0.41	1.19	38.9 ± 2.8
50	26.0	4.20 ± 0.28	8.40 ± 0.55	1.09	29.1 ± 2.4
10	22.0			1.018	39.9 ± 2.8
3.6	22.0			1.007	56.3 ± 10.0

$k_f + k_m = (3.35 \pm 0.07) \times 10^6\ s^{-1}$ $\quad k_{iso} = (7.70 \pm 0.05) \times 10^5\ s^{-1}$
$k_q = (1.95 \pm 0.08) \times 10^7\ M^{-1}\ s^{-1}$ [d] $\quad k_2 = (1.42 \pm 0.11) \times 10^6\ M^{-1}\ s^{-1}$

[a] Taken from ref 2. [b] Experimental data averaged from 550 to 770 nm. [c] Ratio of IC_{tot} to IC (eq 6). [d] About 8 times faster than diffusion; however, $k_{diff} \approx 2.3 \times 10^6\ M^{-1}\ s^{-1}$ [2] is not reliable in supercooled liquid states.

SCHEME 1

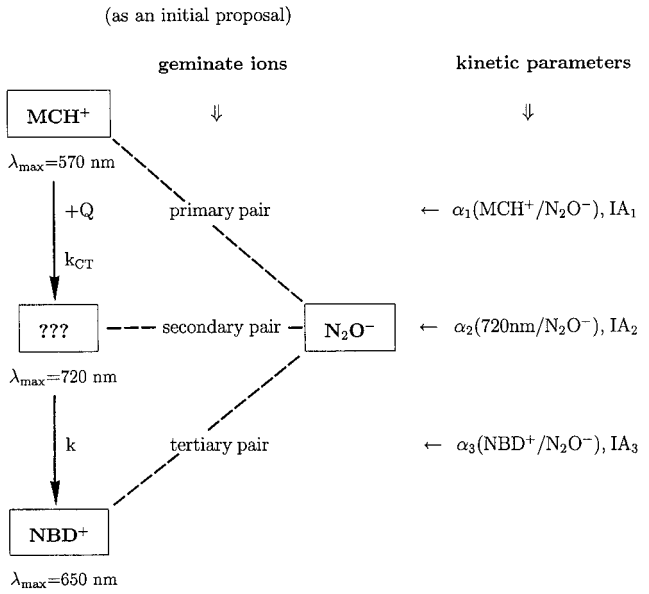

transient spectra in the visible λ range (Figure 1). For concentrations of Q from 200 to 50 mM, a very early 720 nm transient absorption was detected, which shifts within about 300 ns toward 650 nm. The latter band is expected to be due to the norbornadiene cation (NBD^+).[2] This implies that the 720 nm species represents a precursor cation to NBD^+, initially being produced from the solvent radical cation MCH^+ by charge transfer to Q. As MCH^+ is of very high mobility, the buildup of the 720 nm band is beyond the experimental time resolution. For lower concentrations of Q (50−3.6 mM) only the 650 nm band could be seen.

A test for *geminate ion kinetics* is shown in Figure 2 by plotting the absorbance against $t^{-0.6}$. The kinetic behavior is strongly [Q]-dependent: the curve for 100 mM Q is representative for [Q] $\geq$ 50 mM and the curve for 3.6 mM Q for [Q] $\leq$ 10 mM. *At high concentrations* of Q there is an unexpected plateau region ($0.6 < t^{-0.6} < 1.6\ \mu s^{-0.6}$ or between 0.5 and 2.3 μs). The initial decay of the 720 nm species toward the plateau appears to correspond to an apparent first-order decay with $k_{app} \approx 7 \times 10^6\ s^{-1}$, independent of λ from 550 to 800 nm. The final linearity (for $t^{-0.6} \lesssim 0.5\ \mu s^{-0.6}$) is expected to correspond to the geminate ion recombination of NBD^+ with N_2O^- (or O^-). This linearity is [Q]-dependent, due to viscosity variations, as found previously for NBD solutions in MCH.[2] *At low concentrations* of Q the kinetics appears to be very different and rather complex, except that the final linearity again should be due to the NBD^+/N_2O^- recombination.

With methyltetrahydrofuran (MTHF) as a *positive charge scavenger*, the 720 nm band is reduced by 25% with 3 mM or 48% with 20 mM MTHF. There is no effect on the apparent first-order decay rate. The 720 nm species therefore has a positive ion as precursor (the solvent radical cation) but does not react with MTHF (or decays faster than the scavenging process).

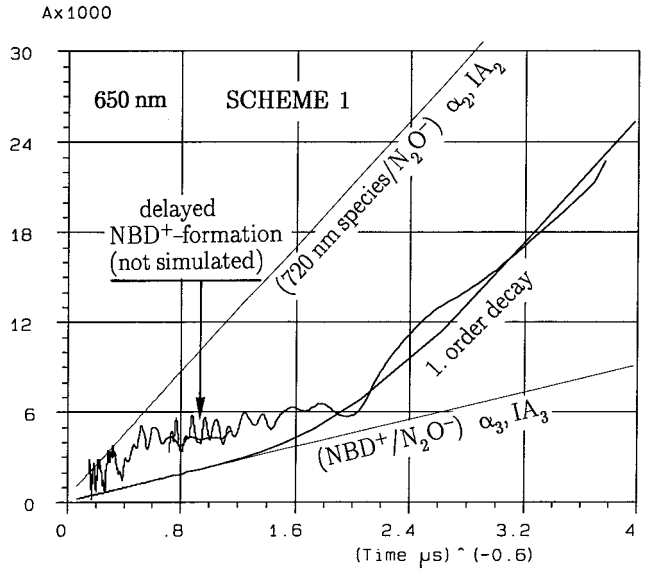

Figure 3. A trial simulation for the rate curve at 650 nm in a solution of 100 mM Q in MCH at 133 K on the basis of Scheme 1. The apparent first-order rate constant for the decay of the "720 nm species" is $k_{app} \approx 7 \times 10^6\ s^{-1}$. However, the simulation for late times (t > 400 ns, means $t^{-0.6} < 1.8\ \mu s^{-0.6}$) is impossible on the basis of Scheme 1.

Focusing on the high concentrations of Q, the results would suggest a mechanism as shown in Scheme 1.

As there is no buildup observable for the 720 nm band, the kinetic simulation can only cover the secondary and tertiary pairs of geminate ions and the corresponding transfer rate k. The mobility values α_2 and α_3 are taken from the system with NBD in MCH[2] (see Table 1). The best possible simulation is shown in Figure 3 for $\lambda_{max}(NBD^+)$. At early times (large $t^{-0.6}$ values) fitting to the experiment is possible with $k_{app} = 7 \times 10^6\ s^{-1}$. For $t^{-0.6} < 1.8\ \mu s^{-0.6}$ (means later than ca. 400 ns) however the simulation is unable to reach experimental values: there must be a delayed production of NBD^+ not covered by Scheme 1. Similar delayed formation of NBD^+ has been reported by J. L. Gębicki et al.[9] for glassy systems. The NBD^+ intercept (IA_3) represents only about 10% (from simulation) or 33% (from experimental curve) from what would be expected in comparison with the measured free ion yield in a NBD/MCH system.[2]

IV. Discussion

If one would like to assign the 720 nm band to the quadricyclane cation Q^+, then the following discrepancies would

SCHEME 2

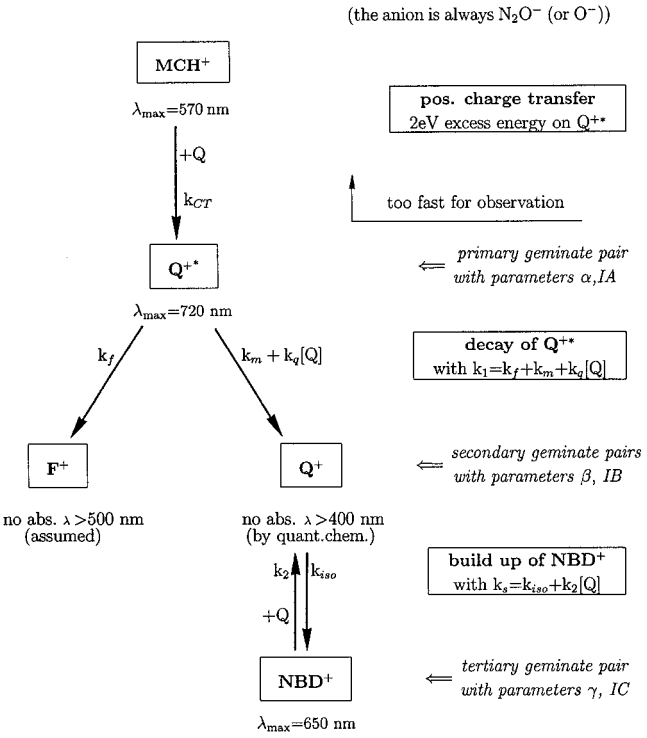

be yielded: (1) Quantum chemistry is unable to predict a visible band near 720 nm for Q^+.[10] (2) The delayed formation of NBD^+ remains unexplained. (3) Q^+ isomerization to NBD^+ is not quantitative; there is a missing yield. The initial reaction Scheme 1 needs to be extended: (1) by introducing a nonabsorbing Q^+ between the 720 nm transient cation and NBD^+, (2) by allowing the 720 nm precursor ion to fragment (or isomerize), in competition with producing Q^+, and (3) by accepting that NBD^+ reacts with Q to re-form Q^+ (I_p(NBD) = 8.43 eV, I_p(Q) = 7.86 eV). The result is shown in Scheme 2.

The precursor ion of Q^+ (λ_{max} = 720 nm) is tentatively called Q^{+*}, as it appears to be of higher energy than Q^+ (see later). It is produced from the solvent radical cation MCH^+ by charge transfer to Q and reacts to form Q^+ with a (pseudo)-first-order rate ([Q]-dependent). The fragment ion F^+ could also be an isomer of Q^+ and is assumed not to absorb in the visible λ range (λ > 500 nm). Such fragmentation (or isomerization) of the quadricyclane cation to F^+ so far has been reported in the literature.[16] It appears to occur from the higher energy state Q^{+*} as it does not occur with photoionization.[12]

Kinetic Analysis with Scheme 2. The nonabsorbing Q^+ separates kinetically the fast 720 nm decay from the slow NBD^+ buildup. Thereby, Q^+ serves as a temporary, nonobservable storage species, so that the NBD^+ buildup appears delayed. Correspondingly the simulation is separated into two steps: (a) The Q^{+*} decay to the nonabsorbing Q^+ with $k_1 = k_f + k_m + k_q$[Q] defining the rate curve at early times (typically for $t^{-0.6} \gtrsim 2\ \mu s^{-0.6}$ or $t \lesssim 300$ ns). k_q describes the [Q]-dependent rate and k_m the constant decay rate to Q^+ (e.g., by the medium). (b) The buildup of NBD^+ from the nonabsorbing Q^+ with $k_s = k_{iso} + k_2$ [Q]. The Q^+ isomerization to NBD^+ (k_{iso}) and its back reaction with Q (k_2) represent a two-way first-order system.

The actual two-step procedure goes first by step b and then by step a: *For late times* ($t^{-0.6} \lesssim 1.4\ \mu s^{-0.6}$) the reaction $Q^+ \rightarrow NBD^+$ with k_s exclusively defines the experimental rate curve. Therefore, the fitting has to start with step b. The geminate ion recombination kinetics for Q^+/N_2O^- is given by β, IB with IB = 0 (no absorption), and that for NBD^+/N_2O^- is given by γ, IC. IC is the contribution of NBD^+ to the free ion spectrum (in equilibrium with Q^+). *For early times* ($t^{-0.6} > 1.4\ \mu s^{-0.6}$) the difference between the experimental curve and the above simulation for $Q^+ \rightarrow NBD^+$ defines the Q^{+*} decay process with k_1. For this simulation (step a) the geminate recombination kinetics for Q^{+*}/N_2O^- is given by α, IA and that for Q^+/N_2O^- again by β, IB with IB = 0 (no absorption).

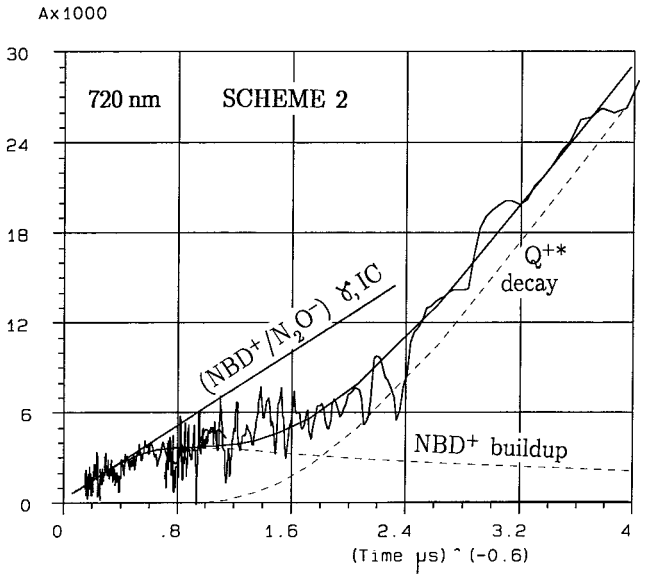

Figure 4. Simulation of a typical rate curve at 720 nm ([Q] = 100 mM) on the basis of Scheme 2. The parameters are $\alpha = \beta = \gamma = 26.7\ \mu s^{0.6}$ (taken from ref 2; see Table 1), k_1 (Q^{+*} decay) = $5.2 \times 10^6\ s^{-1}$, k_s (NBD^+ buildup) = $8.5 \times 10^5\ s^{-1}$, and the free ion intercepts IA(Q^{+*}) = 0.42×10^{-3}, IB(Q^+) = 0, and IC(NBD^+) = 0.23×10^{-3}.

The *mobility values* α, β, *and* γ are all expected to be governed by diffusion and are therefore set identical to the values derived for NBD^+/N_2O^- in a similar NBD−MCH solution[2] (see Table 1). For 100 mM Q at 133 K $\alpha = \beta = \gamma = 26.7\ \mu s^{0.6}$. The real fitting parameters are IA and k_1 for step a and IC and k_s for step b, all being [Q]-dependent. Figure 4 illustrates such a simulation.

The rate constants k_1 *and* k_s were determined for [Q] = 200, 100, and 50 mM at about six wavelengths between 550 and 770 nm. Their averaged values, $\bar{k}_1$([Q]) and $\bar{k}_s$([Q]), are given in Table 1. From $\bar{k}_1 = k_f + k_m + k_q$[Q] and $\bar{k}_s = k_{iso} + k_2$[Q] the following rate constants were derived (Table 1).

$$\text{from } k_1: \quad k_f + k_m = (3.35 \pm 0.07) \times 10^6\ s^{-1}$$

$$k_q = (1.95 \pm 0.08) \times 10^7\ M^{-1}\ s^{-1}$$

$$\text{from } k_s: \quad k_{iso} = (7.70 \pm 0.05) \times 10^5\ s^{-1}$$

$$k_2 = (1.42 \pm 0.11) \times 10^6\ M^{-1}\ s^{-1}$$

To determine k_m (the [Q]-independent relaxation or isomerization to Q^+), k_f is derived from the total yield IC_{tot} (%) (Table 1) for the Q^+/NBD^+ channel (see below) by

$$\frac{IC_{tot}\,(\%)}{100} = \frac{k_1 - k_f}{k_1} \tag{5}$$

The resulting k_f values for [Q] ≥ 50 mM are very similar to the above value for $k_f + k_m$. It is concluded that $k_m \ll k_f$. An absolute value for k_m is hidden within the error limits. This means that Q^{+*} only reacts with Q (by quenching?) in competi-

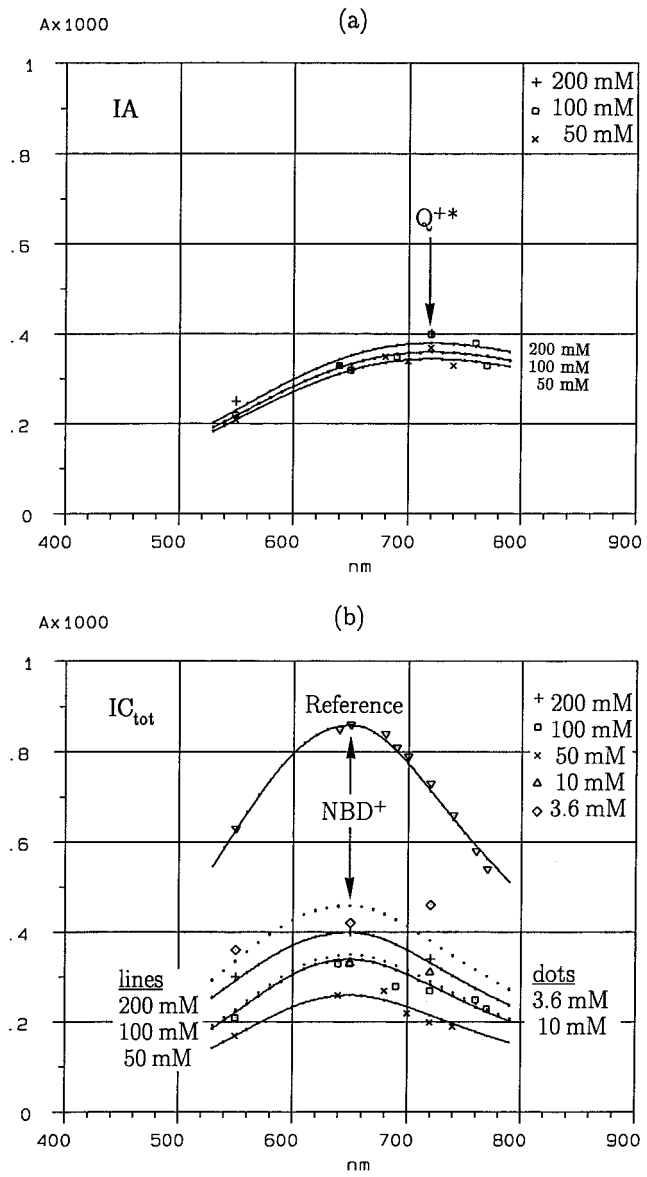

Figure 5. Free ion intercept spectra: (a) IA for Q^{+*} and (b) IC_{tot} for NBD^+ (total yield in the Q^+/NBD^+ channel) as a function of [Q]. The slight [Q]-dependence of IA(Q^{+*}) corresponds to expectation (see later, Figure 7). The [Q]-dependence of $IC_{tot}(NBD^+)$ passes through a minimum near 50 mM. The increase in IC_{tot} at low [Q] is not explainable by Scheme 2 (see later, Figure 6). The reference IC is taken from a solution of 100 mM NBD in MCH.[2] It corresponds to 97% of the free ion yield (3% loss due to $MCHene^+$ production; see Figure 7).

tion with the fragmentation (or isomerization) to F^+. There is therefore no relevant relaxation with the medium, nor any quenching with N_2O ([N_2O] = constant).

The intercept IA represents the free ion contribution of Q^{+*} as shown in Figure 5a. The spectra indicate very little [Q]-dependence. This is explainable in the context of Scheme 3.

The intercept IC corresponds to the free ion contribution of the NBD^+, which finally stays in equilibrium with Q^+. The total free ion yield in the Q^+/NBD^+ channel (expressed in NBD^+ absorbance) then is

$$IC_{tot} = IC\frac{k_{iso} + k_2[Q]}{k_{iso}} \qquad (6)$$

In Figure 5b the data are compared with the total free ion yield

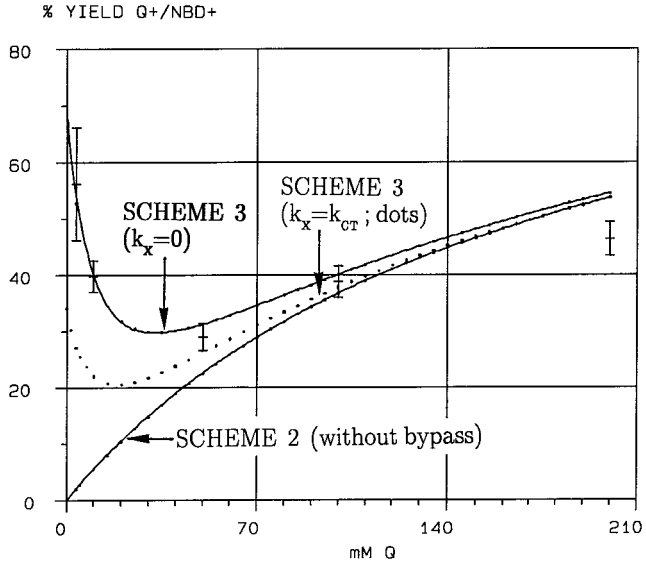

Figure 6. Total free ion yield in the Q^+/NBD^+ channel (expressed as IC_{tot}) in percent of the reference IC of Figure 5. The points represent average values, the error bars the spread of the experimental points. The simulations are based on Schemes 2 and 3, the latter for two values of k_x. Only Scheme 3 with $k_x = 0$ fits to the experimental data at low [Q]. The simulated data for [Q] = 0 are actually for [Q] $\approx 10^{-5}$ M to ascertain total scavenging of all free ions.

SCHEME 3

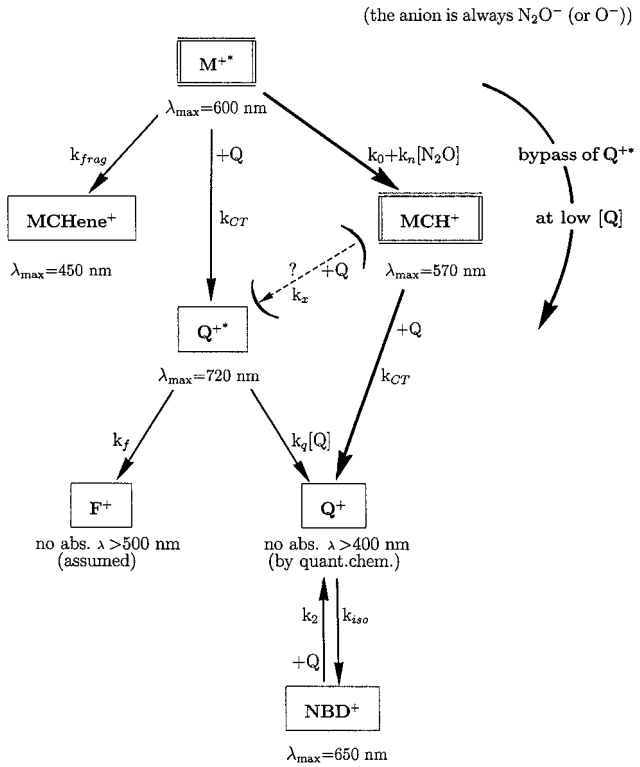

of NBD^+ from a reference system of 100 mM NBD in MCH,[2] where theoretically 97% of the free ion yield should turn up as NBD^+ (3% loss to $MCHene^+$; see Scheme 3). The relative yields expressed in percent are averaged over about six different wavelengths. The results are given in Table 1 as IC_{tot} (%) and shown in Figure 6. The yield never reaches 100%. The missing part must be due to the loss toward F^+ (an isomer or fragment cation). On the basis of Scheme 2 and the rate constants derived above, the simulation of IC_{tot} (%) is calculated and represented in Figure 6 as the curve labeled "SCHEME 2". The cor-

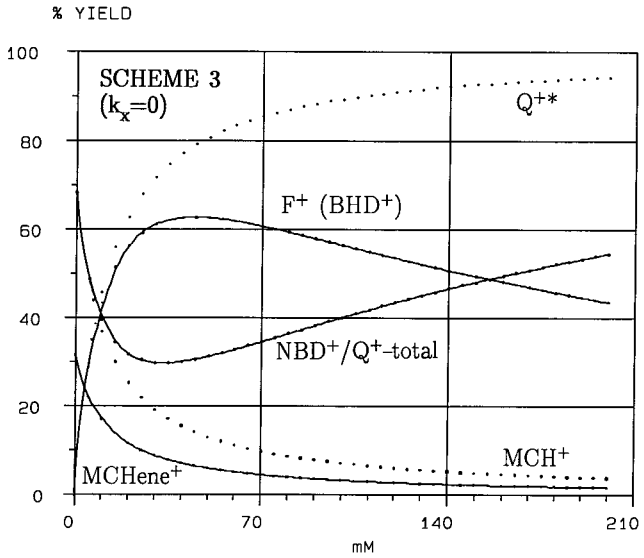

Figure 7. Percent weight of the various reaction channels of Scheme 3. In the first step $MCHene^+$, Q^{+*}, and MCH^+ are produced. In the second step Q^{+*} and MCH^+ (dashed lines) are further split into F^+ and the equilibrium channel Q^+/NBD^+. The curve for MCH^+ reflects the importance of the bypass of $Q^{\bullet+}$ at low [Q]. For the simulated data at [Q] = 0, see the comment in Figure 6.

respondence with the experimental points is reasonable for [Q] ≥ 50 mM. At lower concentrations however the prediction is systematically wrong. The strong yield increase with very low concentration cannot be explained with Scheme 2. At low [Q] there must be an additional path to form NBD^+, active at very low concentrations of Q only.

It is concluded that there is a *need for a bypass of* Q^{+*} to avoid the loss toward F^+ at low concentrations. One also must remember that there is a precursor cation, M^{+*}, to MCH^+.[3] The two solvent cations might have different reactivities toward Q, so far neglected in Scheme 2.

In Scheme 3 MCH^+ of Scheme 2 is replaced by the precursor reaction $M^{+*} \rightarrow MCH^+$, including its fragmentation to the olefinic cation methylcyclohexene$^+$ ($MCHene^+$). At first Q^{+*} is allowed to be produced from both solvent cations: M^{+*} and MCH^+.

Simulation of Scheme 3. The positive charge transfer from both solvent radical cations to Q is governed by their mobility, and the rate constants are therefore set equal to k_{CT} (taken from a NBD/MCH system[2]). All other rate constants are from the results in Scheme 2 (50 mM ≤ [Q] ≤ 200 mM). There are *no new fitting parameters!*

The total free ion yield in the NBD^+/Q^+ channel (IC_{tot} (%)) was recalculated for Scheme 3. The result is shown in Figure 6 as the curve labeled "SCHEME 3 (k_x=k_{CT})". This curve is unable to reproduce the experimental data for [Q] < 50 mM. It is concluded that $k_x \ll k_{CT}$. The simulation with $k_x = 0$ fits best to the experimental points. Therefore, MCH^+ almost exclusively yields Q^+, and Q^{+*} is produced from M^{+*} only. In other words, the difference of 2 eV in ionization potentials between I_p (MCH = 9.85 eV and I_p(Q) = 7.86 eV is not enough energy to produce $Q^{\bullet+}$. The state of the precursor ion Q^{+*} obviously is of higher energy than Q^+. As the fragmentation originates from this Q^{+*} only, it is clear that ionization methods with lesser energy fail to yield F^+. Actually Ishiguro et al.[12] reported that laser photoionization does not produce F^+. F^+ is expected to be the cation of bicyclo[3.2.0]hepta-2,6-diene (BHD^+), another isomer of quadricyclane, as reported by Williams et al.[16] Their statement that the BHD^+ yield strongly

SCHEME 4

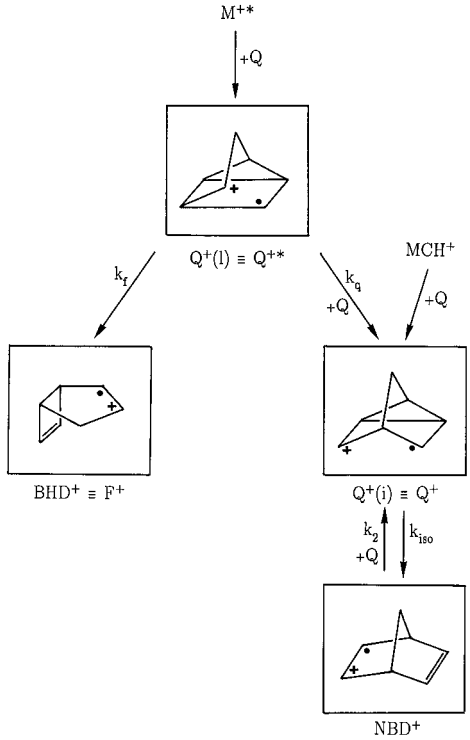

increases with lowering [Q] corresponds rather well with the behavior of F^+ (BHD^+), as seen in Figure 7 down to ca. 50 mM Q.

Weight of the Various Reaction Channels. From the rate data, the weight of the various reaction channels may be calculated as a function of [Q]. In the first step $MCHene^+$, Q^{+*}, and MCH^+ are produced. In the second step Q^{+*} and MCH^+ are further split into F^+ and the equilibrium channel Q^+/NBD^+. The corresponding percent yields are shown in Figure 7. The curve for MCH^+ represents the importance of the bypass for low [Q]. The curve for Q^+/NBD^+ is the same as that in Figure 6 labeled "SCHEME 3 (k_x=0)". The calculated weights are best represented by the corresponding free ion yields.

Simulation of the Rate Curves at Low [Q]. All rate constants so far have been derived from experiments with higher concentrations ([Q] ≥ 50 mM). It would be of interest to test the kinetics for low [Q] as well (a typical low-[Q] rate curve is shown in Figure 2). In this concentration range the bypass channel via MCH^+ is dominant. For the sequence $M^{+*} \rightarrow MCH^+ \rightarrow Q^+ \rightarrow NBD^+$ all steps adopt similar rates (τ in microseconds), and they all suffer simultaneous geminate ion recombination. The $t^{-0.6}$ kinetic method is unable to handle such complex behavior. Qualitatively the rate curves however correspond to expectation.

Absorption Coefficients. From the free ion intercepts (IA for Q^{+*} and IC for NBD^+) and the known G_{fi} (133 K) = 0.06 ± 0.015 $(100\ eV)^{-1}$ the absorption coefficients may be estimated, knowing the corresponding yields from the reaction scheme. The intercepts IA from Figure 5a at λ_{max} = 720 nm are correlated with the calculated yields, as shown in Figure 7 and then averaged over the three concentrations 200, 100, and 50 mM Q. The result is

$$\epsilon_{max}(Q^{+*}) = 380 \pm 20\ M^{-1}\ cm^{-1}$$

The intercept IC in Figure 5b for the NBD^+ reference at λ_{max}

TABLE 2: Characteristics of the Precursors M^{+*} and Q^{+*}

	M^{+*}	Q^{+*}
identification	spectrum with $\lambda_{max} = 600$ nm [2] and $\epsilon_{max} = 700 \pm 50$ M^{-1} cm^{-1} [3] observed through kinetic simulation	spectrum with $\lambda_{max} = 720$ nm and $\epsilon_{max} = 380 \pm 30$ M^{-1} cm^{-1} (Figure 5a) observed for [Q] $\geq$ 50 mM at 133 K (Figure 1) and through kinetic simulation (Figure 5a)
natural lifetime	310 ns at 143 K[3] defined by fragmentation (k_{frag}) and relaxation (k_0)	300 ns at 133 K defined by fragmentation/isomerization (k_f)
quenching ($\rightarrow$ relaxed ion)	by N_2O[3] or $CHCl_3$[4]	by Q (may be charge transfer) *not* by N_2O ($k_m \approx 0$)
relaxation	ca. 10% yield (or less)[3]	almost negligible, as $k_m \ll k_f$
fragmentation	to $MCHene^+$ [2,3] without quencher at least 90% yield	to F^+: most likely BHD^+, an isomer of Q^+
formation	by radiolysis (primary product) responsible for at least 90% of all cationic processes[3]	from M^{+*} by charge transfer to Q *not* from relaxed MCH^+, *not* by laser photoionization[12] Q^{+*} represents a higher energy state than Q^+
reactions	with Q to form Q^{+*} by charge transfer	with Q to form relaxed Q^+ (quenching or charge transfer)

$= 650$ nm [2] yields

$$\epsilon_{max}(NBD^+) = 780 \pm 60\ M^{-1}\ cm^{-1}$$

For both ϵ values the error limits of the G_{fi} value has been ignored. It would affect all absorption coefficients systematically.

Precursor Ions M^{+*} and Q^{+*}. It is surprising that both alkane radical cations, MCH^+ and Q^+, have precursors (M^{+*} and Q^{+*}). Their behaviors have many similarities. Both behave like excited states, as they appear to be quenchable (M^{+*} by N_2O or $CHCl_3$, Q^{+*} by Q), and both undergo fragmentation (or isomerization). Even though their natural lifetimes (defined mainly by k_{frag} and k_f) are too long for electronically excited states, their behavior suggests a higher energy state. In Table 2 the characteristics of the two precursors are summarized.

Adam et al.[6] recently have assigned two distinct structures to the quadricyclane radical cation: $Q^+(l)$, a π-type structure, where the *lateral* bonds are oxidized, and $Q^+(i)$ a σ-type structure with the *internal* bonds being oxidized. $Q^+(l)$ produces the isomer BHD^+ and isomerizes to $Q^+(i)$ in competition, whereas $Q^+(i)$ exclusively isomerizes to NBD^+. $Q^+(l)$ is of higher energy than $Q^+(i)$.

Comparing our kinetic results with the findings by Adam et al. suggests to assign our Q^{+*} to $Q^+(l)$, the π-complex, and our Q^+ to $Q^+(i)$, the σ-type structure. This is shown in Scheme 4. Whether the π-complex really absorbs with $\lambda_{max} = 720$ nm is a subject for theoretical treatment. Our F^+ then corresponds to BHD^+. The rearrangement from $Q^+(l)$ to $Q^+(i)$ with Q might be a charge-transfer process (see Table 2).

The precursor M^{+*}, which is responsible for the production of Q^{+*}, must also represent a higher energy state relative to MCH^+; however, its structure is not understood so far.

Acknowledgment. Support by the Swiss National Science Foundation and by the Research Funds of the ETH Zürich is gratefully acknowledged.

References and Notes

(1) Bühler, R. E. *Res. Chem. Intermed.* **1999**, *25*, 259. Due to fateful printing errors (the publishers do not permit proofreading by authors), ask the author for a corrected reprint.
(2) Katsumura, Y.; Azuma, T.; Quadir, M. A.; Domazou, A. S.; Bühler, R. E. *J. Phys. Chem.* **1995**, *99*, 12814.
(3) Bühler, R. E.; Katsumura, Y. *J. Phys. Chem. A* **1998**, *102*, 111.
(4) Bühler, R. E. *J. Phys. Chem. A* **1999**, *103*, 4986.
(5) Quadir, M. A. Thesis, ETH Zürich, No. 11075, 1995.
(6) Adam, W.; Heidenfelder, T.; Sahin, C. *J. Am. Chem. Soc.* **1995**, *117*, 9693.
(7) Ishiguro, K.; Khudyakov, I. V.; McGarry, P. F.; Turro, N. J., Roth, H. D. *J. Am. Chem. Soc.* **1994**, *116*, 6933.
(8) Roth, H. D. *Acc. Chem. Res.* **1987**, *20*, 343.
(9) Gębicki, J. L.; Gębicki, J.; Mayer, J. *Radiat. Phys. Chem.* **1987**, *30*, 165.
(10) Bally, T. University of Freiburg, Switzerland, private communication, 1993. Calculation based on CASPT2.
(11) van den Ende, C. A. M.; Warman, J.; Hummel, A. *Radiat. Phys. Chem.* **1984**, *23*, 55.
(12) Bartczak, W. M.; Hummel, A. *Radiat. Phys. Chem.* **1994**, *44*, 335.
(13) Bühler, R. E. *Can. J. Phys.* **1990**, *68*, 918.
(14) Bühler, R. E. *Proceedings of the Trombay Symposium on Radiation and Photochemistry TSRP 98*; Bhabha Atomic Research Centre: Trombay, Mumbai, India, Jan 14−19, 1998; Part II, p 429.
(15) Hurni, B.; Brühlmann, U.; Bühler, R. E. *Radiat. Phys. Chem.* **1975**, *7*, 499.
(16) Chen, G.-F.; Wang, J. T.; Williams, F.; Belfield, K. D.; Baldwin, J. E. *J. Am. Chem. Soc.* **1991**, *113*, 9853.